Towards Development of a Self-Healing Composite using a Mendable Polymer and Resistive Heating

Jong Se Park,[1,]* Kosuke Takahashi,[4] Zhanhu Guo,[1] Ying Wang,[1]
Ed Bolanos,[3] Christine Hamann-Schaffner,[3] Erin Murphy,[3]
Fred Wudl[3,5] and H. Thomas Hahn[1,2]

[1]*Department of Mechanical and Aerospace Engineering, University of California
Los Angeles 420 Westwood Blvd., Los Angeles, CA 90095, USA*

[2]*Department of Material Science and Engineering, University of California
Los Angeles 420 Westwood Blvd., Los Angeles, CA 90095, USA*

[3]*Department of Chemistry and Biochemistry, University of California
Los Angeles 420 Westwood Blvd., Los Angeles, CA 90095, USA*

[4]*Department of Mechanical Sciences and Engineering
Tokyo Institute of Technology, Japan*

[5]*Department of Chemistry and Biochemistry, University of California
Santa Barbara, CA, USA*

ABSTRACT: Mendomers are a group of polymers that are mendable upon heating. Specifically, cracks in these polymers have been shown to heal themselves when heated close to the glass transition temperature. The main mechanism behind the healing is the thermally reversible Diels–Alder reaction, where a dicyclopentadiene unit in the polymer backbone breaks apart into two cyclopentadiene terminal groups, which then reunite upon heating. The present study investigates the feasibility of using a mendomer as a matrix for re-mending composites reinforced with graphite fibers. The graphite fibers are used as electrical conductors to provide the necessary heat to the polymer. Specimens were prepared by spreading a monomer, called mendomer, powder on a graphite/epoxy laminate substrate and curing in a vacuum oven. Microcracks were introduced by bending the substrate coupon, and the latter was heated by applying electric currents. The healing behavior was confirmed by disappearance of microcracks that were observed with an optical microscope and a scanning electron microscope (SEM).

KEY WORDS: self-healing composite, microcrack, thermally mendable polymer.

---

*Author to whom correspondence should be addressed. E-mail: jongsepark@ucla.edu
Figures 3, 5, 6 and 8 appear in color online: http://jcm.sagepub.com

INTRODUCTION

T HE CONCEPT OF self-healing involves a damaged material/structure undergoing autonomous repair with minimal external intervention, analogous to the healing process in living organisms. A self-healing material/structure would be more reliable and longer lasting with reduced maintenance costs [1]. Currently, there are two major types of healing techniques. One is based on the use of micro-containers, such as hollow tubes [2–4], hollow fibers [5–7], particles [8], and microcapsules [9–13], to store healing agents. The other uses cross-linked polymers with re-mending capability [20]. The present article is concerned with the latter.

The first report on the synthesis of cross-linked polymers through the thermally reversible Diels–Alder (rDA) cycloaddition was in 1979 by Kennedy and Castner [14]. Since then many studies in this field have followed [15–19]. Chen et al. [20] prepared a truly 're-mending' polymeric material using a multi-diene and multi-dienophile rDA reaction.

These mendable polymers possess several advantages over other self-healing techniques. The polymers by themselves constitute the necessary components for healing, eliminating the need for catalysts or healing agents. As a consequence, the healing process does not bring additional compounds to the system that may compromise the structural properties of the host material. Moreover, these polymers exhibit the ability to heal repeatedly when stimulated by multiple cycles of heating.

The mendomer 401 used in the present work is similar in its structure and healing mechanisms to the one developed by Chen et al. [20]. The thermal properties of the mendomer were characterized by thermogravimetric analysis (TGA) and differential scanning calorimetry (DSC). A small amount of mendomer was applied and cured on a graphite/epoxy laminate coupon and cracks were induced by bending the coupon. Electrical currents were then applied to the coupon to provide the heat necessary to heal the cracks.

EXPERIMENTAL

Material

The chemical structure of mendomer 401, whose name refers to the four carbon atoms, zero nitrogen atoms, and one oxygen atom on the tether chain, is shown in Figure 1,
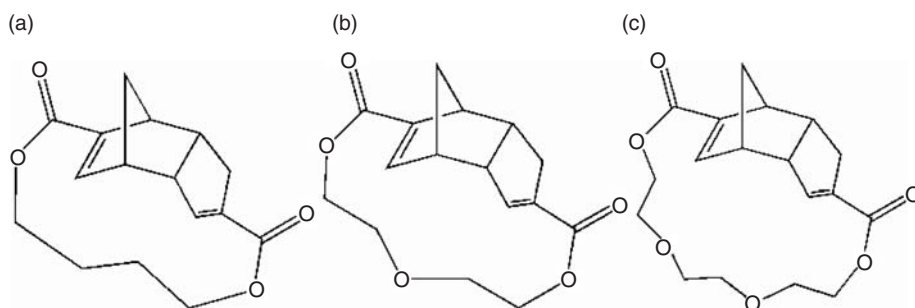

Figure 1. Molecular structures of mendomer series (a) 400, (b) 401, and (c) 602.

along with additional mendomer compounds. Figure 2 shows the polymerization process via the cracking and healing mechanisms at the molecular level. The bonds formed in the Diels–Alder (DA) dicyclopentadiene adduct are the weakest bonds in the polymer chain, and therefore are the breaking point under loading. Fracture occurs through the rDA reaction, resulting in two cyclopentadiene groups at the broken chain ends. However, the DA reaction is thermally reversible, i.e., upon heat treatment and subsequent cooling the broken ends are able to recombine to reform a dicyclopentadiene unit.

Differential Scanning Calorimetry (DSC)

To explore the thermal properties of mendomer 401, dynamic DSC (Perkin Elmer) tests were performed at a temperature ramp rate of 2, 5, 7, 10, and 15°C/min, under a nitrogen flow rate of 20 mL/min, from 25 to 200°C. Since mendomer 401 is a solid powder at room temperature, it was ground into fine particles for the DSC tests.

To study the effect of cure conditions on the glass transition behavior, a small amount of mendomer 401 was cured inside a vacuum oven under three different conditions: 120°C for 3 h, 150°C for 5 h and 150°C for 20 h. The cured mendomer specimens were then crushed into small pieces using a mortar and pestle, and analyzed via DSC at a temperature ramp rate of 10°C/min under 20 mL/min nitrogen flow.

Material Stability

The thermal stability of mendomer 401 was investigated using a Perkin Elmer TGA. The analysis was carried out under an argon flow rate of 50 mL/min at 10°C/min from room temperature to 600°C.

To evaluate the effect of potential oxidation during cure, a small amount of mendomer 401 was cured on a glass plate in an air-circulating oven as well as in a vacuum oven at 120°C for 3 h. After curing, the surfaces of the samples were examined under an optical microscope.

Healing Experiments

About 0.015 g of mendomer 401 powder was cured in a vacuum oven on a graphite/epoxy substrate coupon. The composite laminate was made of AS4/3502 prepreg from Hexcel in a $[0_2/90_2]_S$ lay-up and was 1.2 mm thick. The coupon was 100 mm long and 10 mm wide. A silicone rubber mold with a cavity 5×5 mm was used to localize the mendomer coating at the center of the coupon. Since mendomer 401 has a melting point of 110°C, it was cured at 150°C for 5 h in vacuum. The cured specimen was slowly cooled down to room temperature inside the oven.
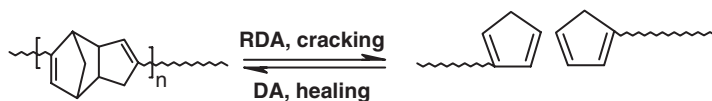
Figure 2. Diels–Alder (cracking) and retro Diels–Alder (healing) reactions of mendomer 401.

Two different methods were used to induce damage in the mendomer coating. In the first method, a razor blade was used to make scratches on the surface. In the second method, a 4411 Instron machine was used to induce microcracks in three-point bending with a maximum strain of 1% strain maintained for 1 min. The required deflection D was calculated using the simple bending equation:

$$D = \frac{L^2}{6d}\varepsilon_f \qquad (1)$$

where L is the beam span (=60 mm), d is the specimen thickness (=1.2 mm), and ε_f is the maximum flexural strain (=1%). The required deflection was thus 5 mm. After the damages were induced, they were verified on an optical microscope.

The mendomer coating was heated through electrical resistive heating of the substrate coupon. In addition, an air-circulating oven was used for convective heating for comparison purposes.

CONVECTIVE HEATING

The specimen with a cracked mendomer coating was placed in an air oven at 110°C for 10 min. After heating, the specimen was slowly cooled to room temperature inside the oven. Special attention had to be paid to the location of the damage since the damage was difficult to detect after healing.

ELECTRICAL RESISTIVE HEATING

For electrical resistive heating, only those specimens with microcracks induced by three-point bending were used to verify the healing ability. To avoid local heating due to high contact resistance at electrodes, electrical copper plating was used to connect the electrodes to the composite coupon surface. The graphite/epoxy substrate coupon was masked using vinyl tape, except for the polished electrodes area, followed by treatment with concentrated sulfuric acid to expose carbon fibers from the epoxy resin. After removing the epoxy resin, the panel was put into the copper sulfate solution for electrodeposition of copper. These freshly prepared copper electrodes were attached with silver paint to stranded wires that were flattened to increase contact area for electrical connection.

To quantify the contact resistance, electrical resistances between two electrodes with distances 15, 30, 45, and 60 mm were measured using a four-probe method to remove the resistance between an alligator clip of the power source and a stranded wire (Figure 3). The resistance results are shown in Figure 4. Since there is no distance between two electrodes at the y intercept of Figure 4, it indicates double the contact resistance between a copper electrode and graphite fibers.

The effective contact resistance of an electrode is $R_{\text{contact}} = 0.138/2 = 0.069\,\Omega$. The resulting effective conductivity in the thickness direction, σ_{contact}, is given by:

$$\sigma_{\text{contact}} = \frac{t}{R_{\text{contact}}S} = \frac{0.1}{0.069 \times (10 \times 10)} = 0.01451/\Omega\,\text{mm} \qquad (2)$$

where t and S are the thickness and area, respectively, of the electrode. Note that the thickness of 0.1 mm is an assumed value.
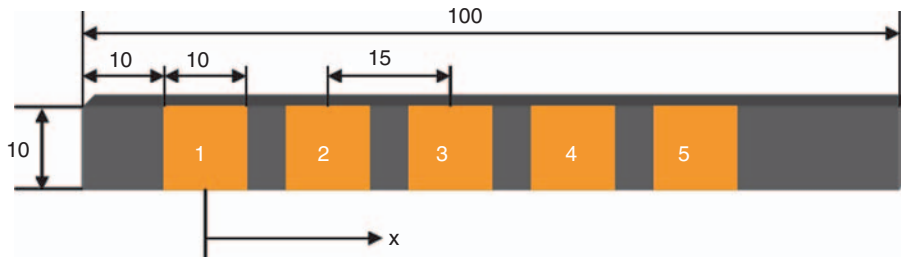
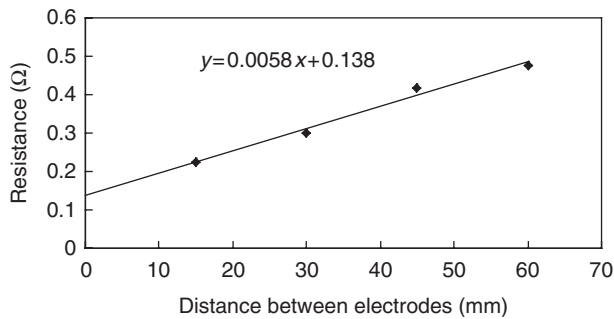**Figure 3.** *Dimensions of a coupon used for measuring contact resistance.*

Figure 4. *Electrical resistances between two electrodes at various distances.*

Table 1. Material properties used in the FE analysis.

Material	Properties	Units	Symbol	Value
GFRP	Electrical conductivity	(1/mm Ω)	σ_0	34.120
			σ_{90}	0.0240
			σ_t	0.0207
	Thermal conductivity	(W/mm K)	λ_0	4.23×10^{-3}
			λ_{90}	0.738×10^{-3}
			λ_t	0.738×10^{-3}
Copper electrode	Electrical Conductivity	(1/mm Ω)	σ_{copper}	59,600
	Thermal Conductivity	(W/mm K)	λ_{copper}	401×10^{-3}
Contact electrode	Electrical Conductivity	(1/mm Ω)	$\sigma_{contact}$	0.0145
	Thermal Conductivity	(W/mm K)	$\lambda_{contact}$	0.5×10^{-3}
Air	Ambient temperature	(K)		298
	Joule heat fraction			1.0
	Heat transfer coefficient	(W/mm^2 K)	h	11.42×10^{-6}

A finite element (FE) analysis was conducted to predict the required current to reach the healing temperature in the composite specimen. The constants used in the analysis are summarized in Table 1. The electrical conductivities of the composite panel were taken from the work of Abry et al. [21], and the thermal conductivities, from the manufacturer, Hexcel. Typical electrical/thermal properties of copper were used for the copper electrodes,
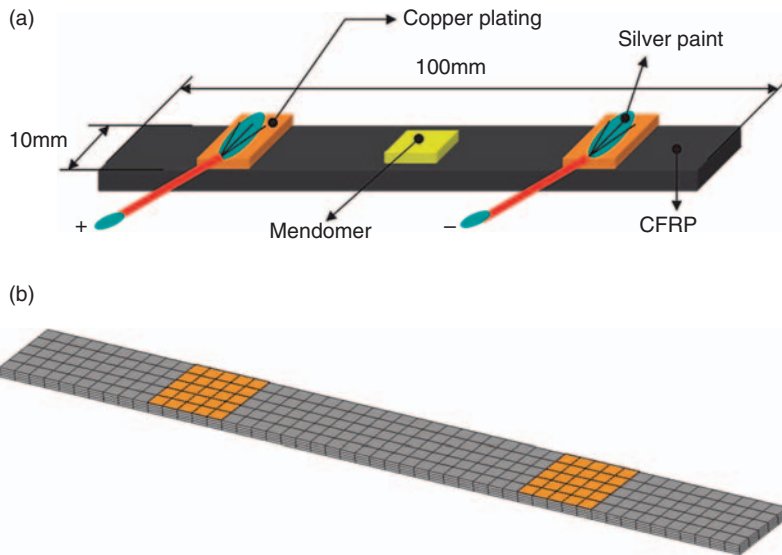
Figure 5. Electrical resistance heating: (a) schematic of experiment and (b) FE model.

and the convective heat transfer coefficient h was taken to be the same as for a heated plate under natural convection [22]. Thermal conductivity of the contact electrodes was assumed to be 0.5 W/mK, which falls between the thermal conductivity of air, 0.03 W/mK, and that of a thermal interfacial material in electronic packaging, 0.7 W/mK [23].

A schematic of the electrical resistance heating is shown in Figure 5. The FE model for the eight-layer $[0_2/90_2]_S$ composite substrate uses 1000 brick elements with four elements in the thickness direction and the electrodes are represented by 25 brick elements with one element in the thickness direction. The steady state electrical/thermal simulation was conducted using the commercial FE software, ABAQUS. A natural convection boundary condition was applied to the top and the bottom surfaces of the composite layers with an ambient temperature of 25°C. A controlled amount of electrical current was applied to the four nodes of the element located at the center of the electrode. The elements located at the same place in the other electrode are set to 0 V. The expected healing temperature is lower than 100°C and it was found to be achievable at a current of 2 A.

During resistive heating experiments, the current and voltage were monitored and the temperature was measured using an infrared thermometer. The current was increased to 2 A and held constant for 20 min before being gradually decreased. After heating, the specimen was cooled down to room temperature. A comparison of the temperature distribution between simulation and experiment is shown in Figure 6.

RESULTS AND DISCUSSION

Melting and Polymerization of Monomer

The DSC graph of mendomer 401 in Figure 7 shows a broad endothermic peak without any sign of an exothermic peak. Earlier results on similar mendomers showed an
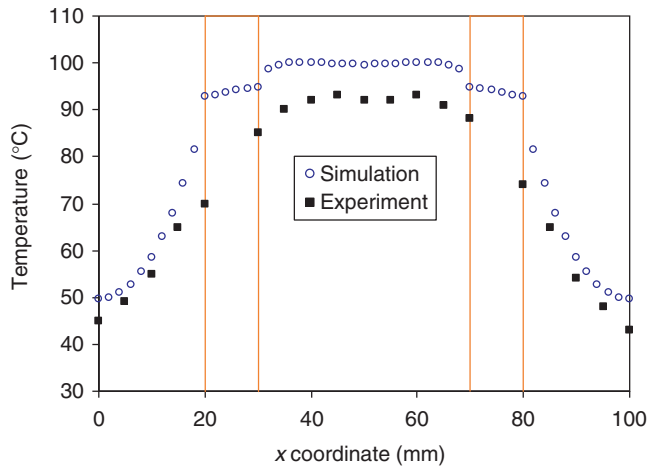
Figure 6. *A comparison of temperature distribution between simulation and experiment.*
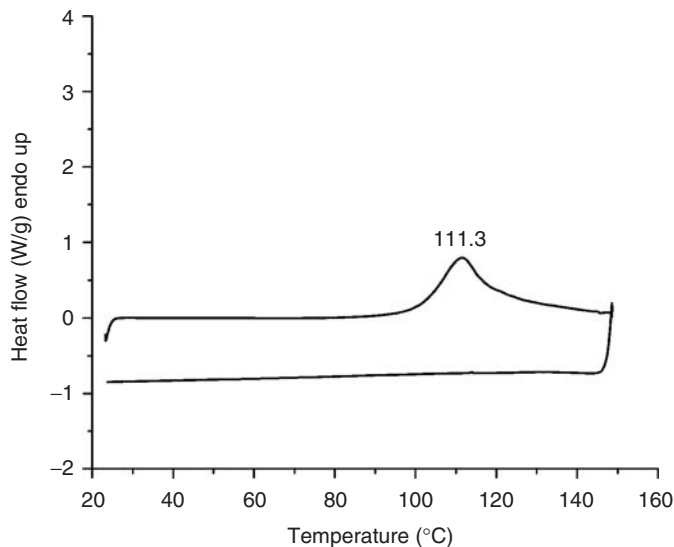

Figure 7. *A typical DSC thermograph of mendomer 401 (10 K/min).*

exothermic peak, although small, immediately following the endothermic peak. It is possible, therefore, that even though the polymerization is exothermic, its evidence in the DSC trace is overshadowed by the strong endothermic melting peak. From the DSC thermograph at a temperature rate of 10°C/min, the melting point of mendomer 401 is seen to be around 110°C with an associated 74.1 J/g heat of fusion.

Dynamic DSC thermographs at various temperature rates are shown in Figure 8. All DSC graphs are very smooth in the beginning of the endothermic reaction, which could be interpreted as the beginning of the melting of mendomer 401 powder. However, with increasing temperature ramp rates, disturbances are observed between 120 and 210°C.
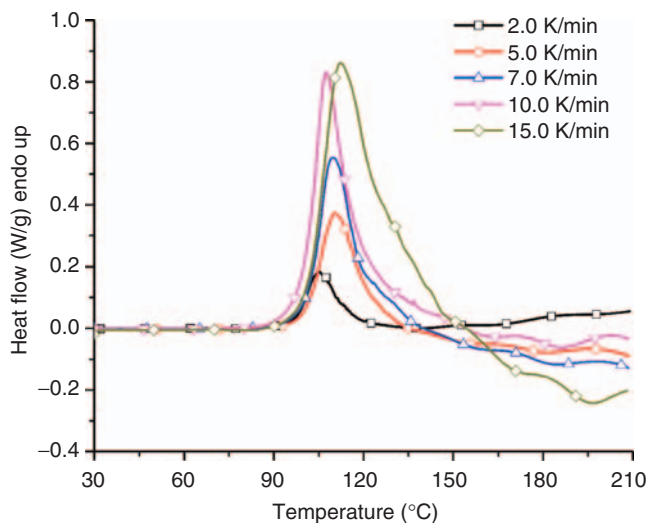
Figure 8. Dynamic DSC thermographs of mendomer 401 with different temperature ramps.

These are likely due to the rDA process. Further experiments are required to establish this with certainty.

Glass Transition and Healing of Polymer

Figure 9 shows the thermographs of mendomer 401 cured under several different conditions. A small endothermic peak with energy 3.1 J/g is found around 54°C during the first run in Figure 9(b), which is presumed to be a glass transition temperature. There is no peak observed during the second heating cycle. The location of the endothermic peak seems to be related to the cure temperature and time. The mendomer specimens that were cured at 150°C for 20 and 5 h, respectively, exhibit a peak around 100 and 60°C; however, those that were cured at 120°C for 3 h have a peak around 40°C. A higher cure temperature and a longer cure time shifts the glass transition to a higher temperature due to higher-degree of the cross-linking in the polymer. The absence of endothermic peaks indicates a full cross-linking (curing) of the polymer.

Material Stability

Figure 10 shows the weight change of mendomer 401 over the temperature range from room temperature to 600°C at 10°C/min. The polymer loses 5% of mass up to 288°C and 50% of mass up to 445°C. Therefore, the material is stable up to 288°C, decomposing above that temperature.

The mendomer cured inside the air-circulating oven was dark yellow (Figure 11(a)), and there were microcracks near the boundary. However, when cured inside a vacuum oven, it was light yellow with no microcracks (Figure 11(b)). The difference is believed to be due to the oxidation of mendomer 401, which interferes with cross-linking and results in shorter molecular chains. Therefore, the polymer should be cured under anaerobic conditions.
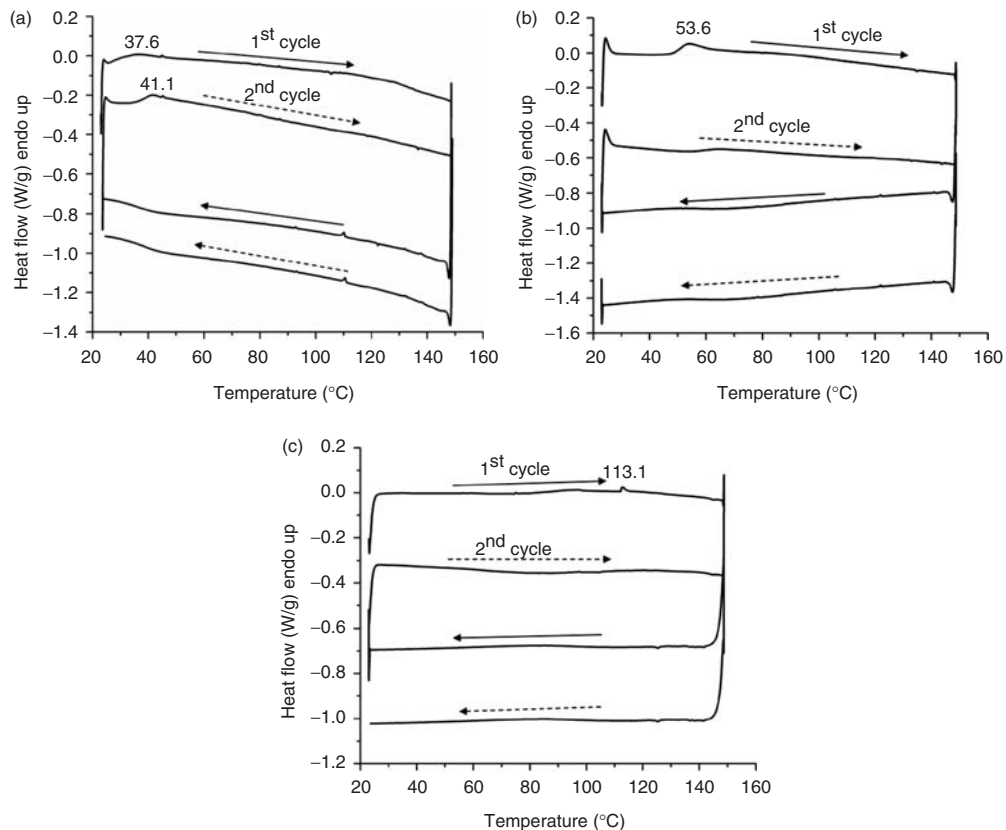
Figure 9. DSC thermographs of mendomer 401 cured at: (a) 120°C for 3 h, (b) 150°C for 5 h, and (c) 150°C for 20 h.
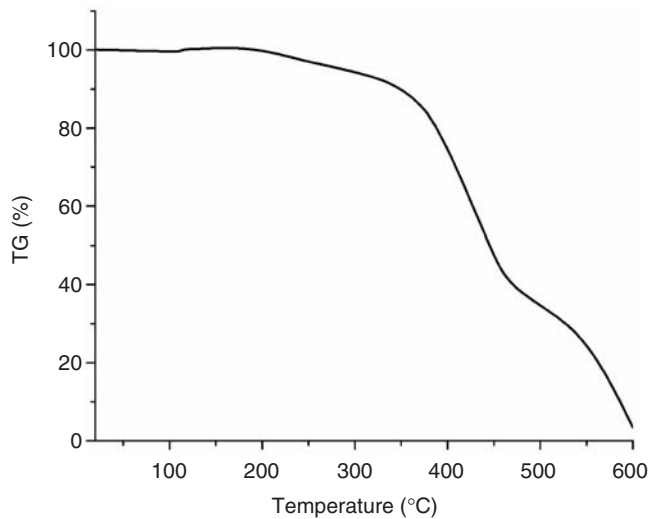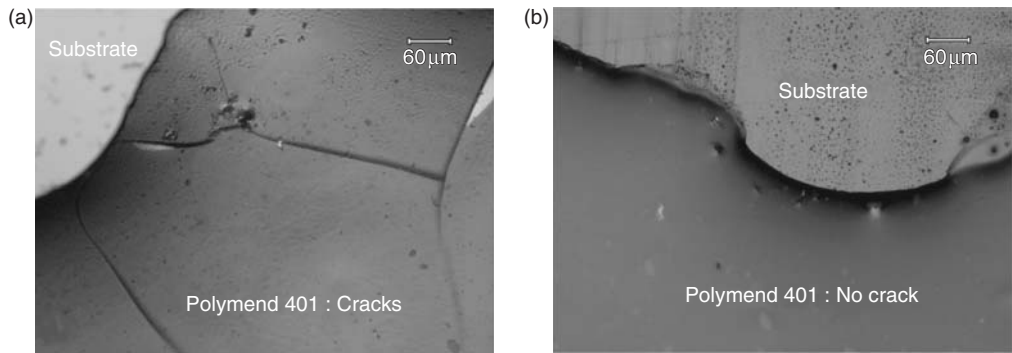

Figure 10. TGA result of mendomer 401.

Figure 11. Mendomer 401 cured in: (a) normal oven and (b) vacuum oven.
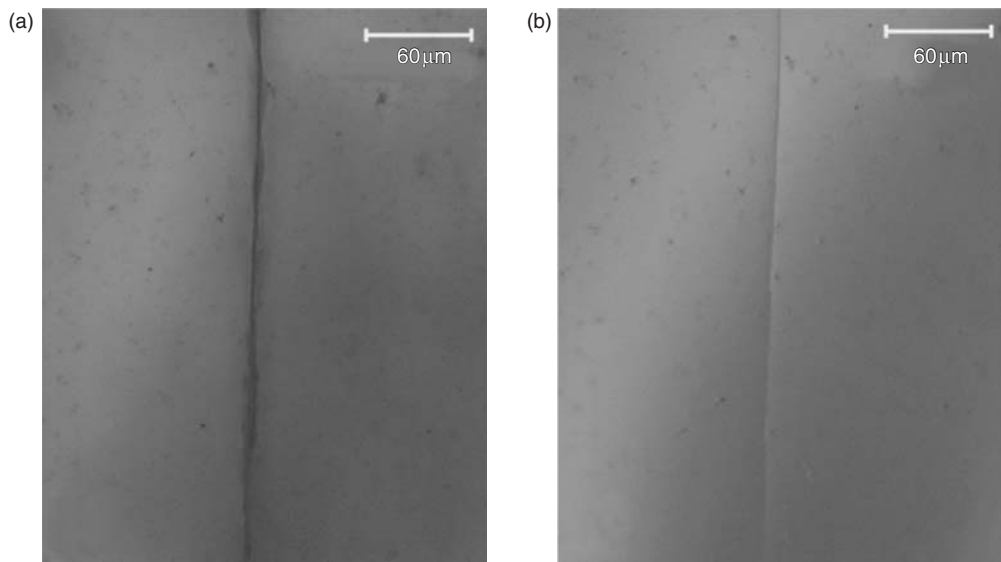

Figure 12. Convective heating of a microcrack: (a) before healing and (b) after healing.

Healing Ability

The microcracks induced by three-point bending were healed well in the air-circulating oven and became almost invisible on the microscope (Figure 12). However, this was not the case with the scratch induced by a razor blade (Figure 13). In the latter case, the damaged surfaces are widely separated and are not in contact with each other across the scratch. This would be a limitation on the healing ability of mendomer 401.

The electrical resistive heating was found to work well with the polymer. Figure 14 shows a crack in the mendomer coating before and after electrical resistive heating of the substrate. Crack healing was observed at a relatively low temperature range of 70–100°C, and was complete within minutes at these temperatures.

To identify the heal morphology, the healed microcracks were examined under a scanning electron microscope (SEM). Figure 15 shows two healed cracks: one healed in the
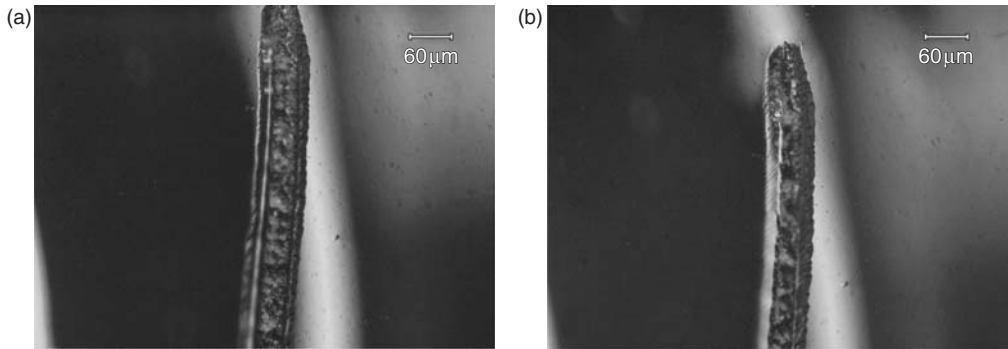
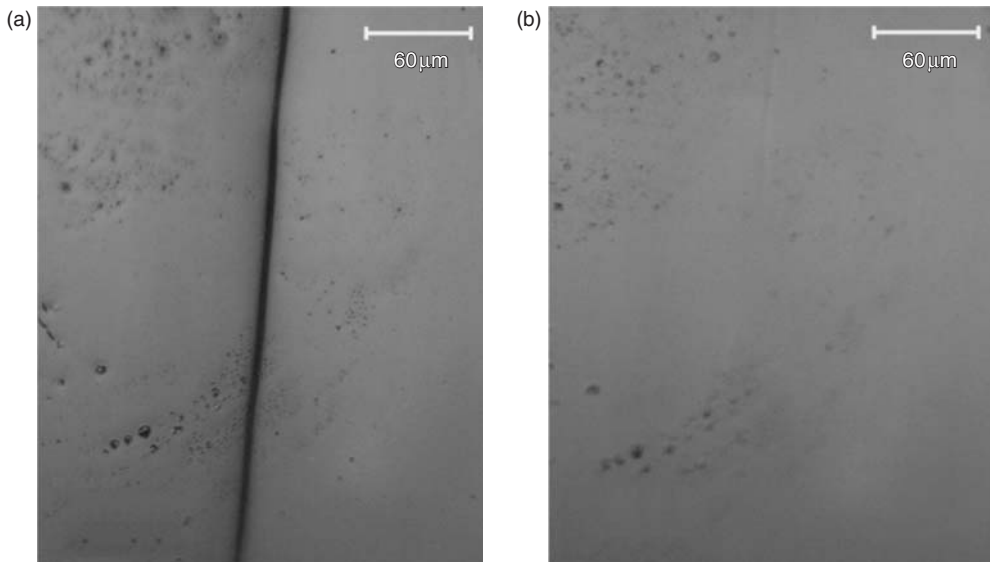***Figure 13.*** *Absence of healing in a razor blade scratch: (a) before healing and (b) after healing.*

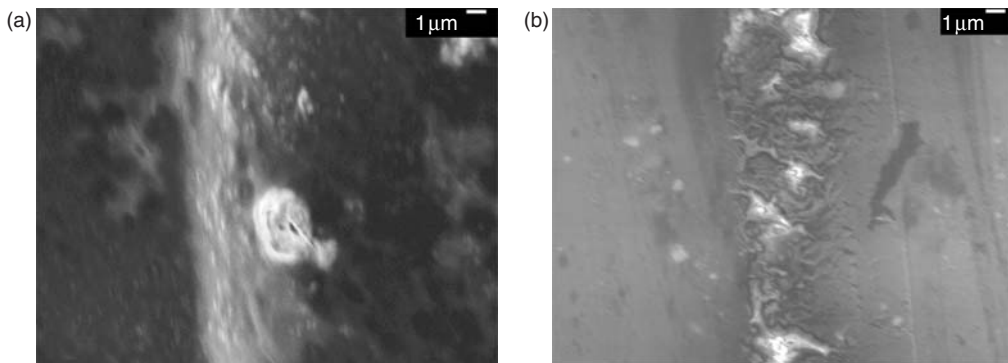***Figure 14.*** *Resistive heating of a microcrack: (a) before healing and (b) after healing.*

Figure 15. *SEM micrographs (×3000) of a crack after healing: (a) convective healing and (b) resistive healing.*

air-circulating oven and the other healed by electroresistive heating. Both cracks are completely closed. However, the former shows more extensive scars than the latter. Although not surprising, it is unclear why these scars are formed, though it can potentially be attributed to a phenomenon akin to surface tension during healing.

CONCLUSIONS

The healing ability of mendomer 401 via electrical resistive heating has been demonstrated by using a graphite/epoxy laminate as a substrate. Microcracks in mendomer coatings on a graphite/epoxy substrate coupon were healed completely when the coupon was heated electrically. Oxidation should be avoided during curing of the polymer; however, it does not affect healing once the polymer is cured.

To use mendomer 401 as a matrix of self-healing composite, there are several questions to be solved. First, mechanical properties which are important to be a good matrix for composite should be studied. Also, healing efficiency that can be defined by ratios of ultimate strength or toughness of the polymer before and after healing should be quantified. Finally, a scaleable manufacturing process of mendomer should be developed for fabrication of a self-healing composite.

Although there is considerable work to be done, mendomer 401 is one of the most attractive candidates as a matrix material for mendable composites according to its healing ability, using graphite fibers network which can provide a health monitoring system in future.

ACKNOWLEDGMENTS

REFERENCES

1. Pang, J.W.C. and Bond, I.P. (2005). A Hollow Fibre Reinforced Polymer Composite Encompassing Self-healing and Enhanced Damage Visibility, *Comp. Sci. Tech.*, **65**: 1791–1799.
2. Dry, C. and McMillan, W. (1996). Three-part Methylmethacrylate Adhesive System as an Internal Delivery System for Smart Responsive Concrete, *Smart Mater. Struct.*, **5**(3): 297–300.
3. Dry, C. (2000). Three Design for the Internal Release of Sealants, Adhesives and Waterproofing Chemical into Concrete to Release, *Cement Concrete Res.*, **30**: 1969–1977.
4. Li, V.C., Lim, Y.M. and Chan, Y.W. (1998). Feasibility Study of a Passive Smart Self-healing Cementitious Composite, *Composites B*, **29**(B): 819–827.
5. Dry, C. (1996). Procedure Developed for Self-repair of Polymer Matrix Composite Materials, *Comp. Struct.*, **35**(3): 263–269.
6. Motuku, M., Vaidya, U.K. and Janowski, G.M. (1999). Parametric Studies on Self-repairing Approaches for Resin Infused Composites Subjected to Low Velocity Impact, *Smart Mater. Struct.*, **8**: 623–638.

7. Bleay, S.M., Loader, C.B., Hawyes, V.J., Humberstone, L. and Curtis, P.T. (2001). A Smart Repair System for Polymer Matrix Composites, *Composites A*, **32**: 1767–1776.

8. Zako, M. and Takano, N. (1999). Intelligent Material Systems using Epoxy Particles to Repair Microcracks and Delamination Damage in GFRP, *J. Int. Mater. Sys. Struct.*, **10**(10): 836–841.

9. White, S.R., Sottos, N.R., Geubelle, P.H., Moore, J.S., Kessler, M.R., Sriram, S.R., Brown, E.N. and Viswanathan, S. (2001). Autonomic Healing of Polymer Composites, *Nature*, **409**: 794–797.

10. Kessler, M.R. and White, S.R. (2001). Self-activated Healing of Delamination Damage in Woven Composites, *Composites A*, **32**: 683–699.

11. Brown, E.N., Sottos, N.R. and White, S.R. (2002). Fracture Testing of a Self-healing Polymer Composite, *Exp. Mech.*, **42**(4): 372–379.

12. Kessler, M.R., Sottos, N.R. and White, S.R. (2003). Self-healing Structural Composite Materials, *Composites A*, **34**: 743–753.

13. Brown, E.N., White, S.R. and Sottos, N.R. (2004). Microcapsule Induced Toughening in a Self-healing Polymer Composite, *J. Mater. Sci.*, **39**: 1703–1710.

14. Kennedy, J.P. and Castner, K.F. (1979). Thermally Reversible Polymer Systems by Cyclopentadienylation. I. A Model for Termination by Cyclopentadienylation of Olefin Polymerization, *J. Polym. Sci., Part A: Polym. Chem.*, **17**: 2039–2054.

15. Canary, S.A. and Stevens, M.P. (1992). Thermally Reversible Crosslinking of Polystyrene via the Furan-Maleimide Diels-Alder Reaction, *J. Polym. Sci., Part A: Polym. Chem.*, **30**: 1755–1760.

16. Engle, L.P. and Wagener, K.B. (1993). Thermally Reversible Polymer Linkages. II. Linear Addition Polymers, *J. Polym. Sci., Part A: Polym. Chem.*, **31**: 865–875.

17. Gousse, C., Gandini, A. and Hodge, P. (1998). Application of the Diels–Alder Reaction to Polymers Bearing Furan Moieties. 2. Diels–Alder and Retro-Diels–Alder Reactions Involving Furan Rings in Some Styrene Copolymers, *Macromolecules*, **31**: 314–321.

18. Jones, J.R., Liotta, C.L., Collard, D.M. and Schiraldi, D.A. (1999). Cross-linking and Modification of poly(ethylene teraphthalate-co-2,6-anthracenedicarboxylate) by Diels–Alder Reactions with Maleimides, *Macromolecules*, **32**: 5786–5792.

19. Imai, Y., Itoh, H., Naka, K. and Chujo, Y. (2000). Thermally Reversible IPN Organic-inorganic Polymer Hybrids Utilizing the Diels–Alder Reaction, *Macromolecules*, **33**: 4343–4346.

20. Chen, X., Dam, M.A., Ono, K., Mal, A., Shen, H.B., Nutt, S.R., Sheran, K. and Wudl, F. (2002). A Thermally Re-mendable Cross-linked Polymeric Material, *Science*, **295**: 1698–1702.

21. Kwok, N. and Hahn, H.T. (2007). Resistance Heating for Self-healing Composites, *J. Comp. Mater.*, **41**: 1635–1654.

22. Abry, J., Bochard, S., Chateauminois, A., Salvia, M. and Girau, G. (1999). *In Situ* Detection of Damage in CFRP Laminates by Electrical Resistance Measurements, *Comp. Sci. Tech.*, **59**: 925–935.

23. Grujicic, M., Zhao, C.L. and Dusel, E.C. (2005). The Effect of Thermal Contact Resistance on Heat Management in the Electronic Packaging, *Appl. Surface Sci.*, **246**: 290–302.